New Mn_{12} single-molecule magnets from edge-sharing bioctahedra

Muralee Murugesu,[a] Wolfgang Wernsdorfer,[b] Khalil A. Abboud,[a] Euan K. Brechin*[c] and George Christou*[a]

Received 2nd December 2005, Accepted 29th March 2006
First published as an Advance Article on the web 19th April 2006
DOI: 10.1039/b517108c

Dodecanuclear Mn clusters based on edge-sharing bioctahedra display the scan-rate- and temperature-dependent hysteresis loops that are indicative of single-molecule magnetism behaviour.

Individual molecules that function as nanoscale magnetic particles are the targets of much current research because they represent a 'bottom up' approach to nanomagnetism with potential applications such as molecule-based high density information storage.[1] In order to function as single-molecule magnets (SMMs), molecules must display slow magnetization relaxation, a property that arises from the combination of a large ground state spin (*S*) and significant magnetoanisotropy (zero-field splitting) of the easy-axis type, manifested as a negative zfs parameter, *D*.[2] The Jahn–Teller (JT) distortion of high-spin Mn(III) in near-octahedral geometry (which yields significant single-ion anisotropy) and the large numbers of polynuclear clusters displaying a large ground state *S* value, make the chemistry of Mn a rich source of SMMs. Indeed, most identified SMMs are compounds of Mn(III) of various nuclearities and structural type, and often mixed valent.[3]

We have a longstanding interest in the study of polynuclear manganese complexes and have developed a wide range of synthetic strategies and methods to both access new cluster families and to manipulate (and enhance the properties of) existing ones.[4] Among such methods have been the reaction of triangular $[Mn_3O(O_2CR)_6(py)_3]^+$ (R = Me, Et, Ph, *etc*; py = pyridine) complexes with chelating ligands such as 2,2′-bipyridine (bpy), 2-hydroxymethylpyridine (Hhmp), and various others, which causes a structural rearrangement to a higher nuclearity product.[4] Another strategy developed recently is 'reductive aggregation' in which a high oxidation state Mn source is dissolved in alcohol (*e.g.* MeOH) in the presence of potential bridging ligands, forcing a reduction of the manganese ions and a resulting structural aggregation to a polynuclear product, with the added possibility of the alcohol providing additional alkoxide (*e.g.* MeO^-) bridging ligands.[5] In the present work, we have combined these strategies by carrying out reactions in an alcohol-containing medium using tripodal alcohol chelating ligands, which we have previously shown to be excellent building blocks for the synthesis of SMMs.[6]

Reaction of $[Mn_3O(O_2CPh_2)_6(py)_3](ClO_4)$ (0.27 g, 0.25 mmol) with H_4peol (pentaerythritol, $C(CH_2OH)_4$) (0.034 g, 0.25 mmol) in MeOH–MeCN afforded the dodecanuclear complex $[Mn^{III}_4Mn^{II}_8(\mu_5\text{-}O)_2(\mu_3\text{-}OMe)_2(Hpeol)_4(O_2CPh_2)_{10}(H_2O)_2]\cdot 6MeCN$ (**1**·6MeCN) in ~60% yield after 2 weeks. An analogous complex, $[Mn^{III}_4Mn^{II}_8(\mu_5\text{-}O)_2(\mu_3\text{-}OH)_2(Hpeol)_4(O_2CPh_2)_{10}(H_2O)_2]\cdot 12MeCN$ (**2**·12MeCN) in ~45% yield was obtained by carrying out the reaction in MeCN alone, although the product takes up to three weeks to crystallise.

Complex **1** crystallizes in the orthorhombic space group *Pbca* with the asymmetric unit containing a half cluster and three MeCN molecules of crystallization.† The cluster consists of a central $[Mn^{III}_4Mn^{II}_6O_2]^{20+}$ unit (Fig. 1), which can be described as two distorted octahedra (Mn1, Mn1a, Mn2, Mn2a, Mn3, Mn3a, Mn5, Mn5a, Mn6 and Mn6a) sharing an edge along the Mn1–Mn1a vector, and with the two remaining Mn(II) ions (Mn4, Mn4a) each capping one face of the octahedra. The Mn(III) ions (Mn1, Mn2 and symmetry equivalents) are at the centre of the cluster, two occupying the apical positions and two the shared edge of the octahedra. They are all six-coordinate in distorted octahedral geometries with their JT elongation axes essentially co-parallel (thicker black bonds in Fig. 1). The Mn(II) ions are also six-coordinate and in distorted octahedral environments, with the exception of Mn6 and Mn6a which are seven-coordinate.

At the centre of both distorted octahedra are rare five-coordinate oxide ions (O6 and O6a). They can be regarded as either square-pyramidal or pseudo-octahedral given the long (3.431(4) Å) contact to the apical Mn (Mn6) sites. The $Hpeol^{3-}$ ligands bridge in an $\eta^3,\eta^3,\eta^2,\mu_5$-fashion spanning a triangular face of one octahedron and further bridging to the apical Mn site on the neighbouring octahedron and the peripheral face-capping Mn ion. This peripheral Mn ions are also each connected to the central octahedra by a μ_3-OMe ligand (or by a μ_3-OH ligand in **2**) and two *syn*,*syn*, μ-O_2CR ligands. The remaining carboxylate groups bridge in two different ways: either between two apical Mn sites on neighbouring octahedra in the usual μ-fashion, or between apical and equatorial Mn ions in the same octahedron in the more unusual η^1,η^2,μ-fashion. Two terminal water molecules complete the coordination of Mn4 and Mn4a.

Since mixed-valent $Mn^{III}_4Mn^{II}_8$ complexes **1** and **2** form from the use of a Mn(III) reagent, we also explored the reaction with a Mn(II) reagent. The reaction of $Mn(O_2CMe)_2\cdot 4H_2O$ (0.18 g, 0.75 mmol) with H_4peol (0.068 g, 0.50 mmol) and NaOH (0.01 g, 0.25 mmol) in MeOH–MeCN led to subsequent isolation of $Na[Mn^{III}_4Mn^{II}_8(\mu_5\text{-}O)_2(\mu_3\text{-}OH)(\mu_3\text{-}OMe)(Hpeol)_4(O_2CMe)_{11}(H_2O)_3]\cdot 4MeCN\cdot H_2O$ (**3**·4MeCN·H_2O) in 45% yield. Complex **3**·4MeCN·H_2O crystallizes in the triclinic space group $P\bar{1}$ with the complex on an inversion centre. It contains an $[Mn_{12}]$ unit very similar to those in **1** and **2**, except two bridging carboxylates are now replaced by three terminal carboxylates and a terminal H_2O, and there is one μ_3-OH^- and one μ_3-OMe^- disordered with equal occupancy. The less bulky acetate groups and the supply of Na^+ ions allow the $[Mn_{12}]$ units to be linked together into a 1-D chain (Fig. 1, bottom) *via* Na^+ ions attached to carboxylate oxygen atoms (O16, O20, O22 and their symmetry equivalents) on adjacent molecules.

The Mn–oxgen core of complexes **1–3** resembles the structural unit found in early transition metal polyoxometalates

[a]*Department of Chemistry, University of Florida, Gainesville, Florida, 32611-7200, USA. E-mail: christou@chem.ufl.edu*
[b]*Laboratoire Louis Néel-CNRS, 38042, Grenoble, Cedex 9, France*
[c]*School of Chemistry, The University of Edinburgh, West Mains Road, Edinburgh, UK EH9 3JJ. E-mail: ebrechin@staffmail.ed.ac.uk*

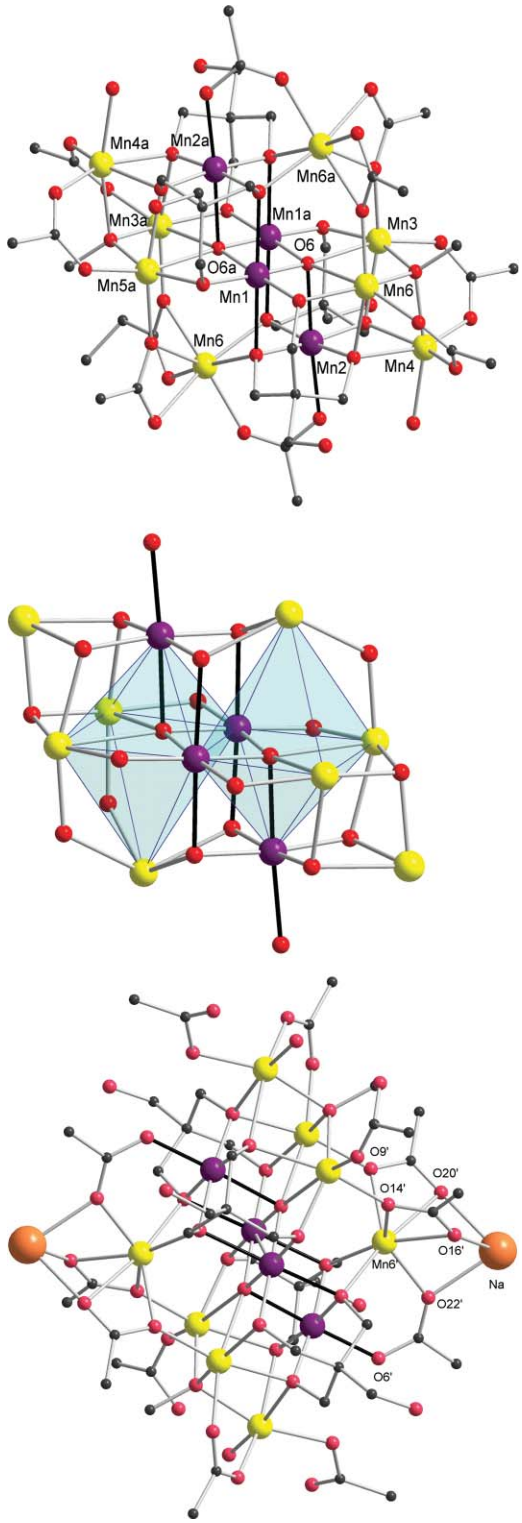

Fig. 1 Structure of the $[Mn_{12}]$ complex **1** (top) and its central core (middle); Mn^{III} Jahn–Teller elongation axes are highlighted as thick black bonds. Phenyl rings and H atoms have been omitted for clarity. (bottom) A short section of the 1-D chain of Na^+-bridged $[Mn_{12}]$ units of complex **3**. Mn^{III} purple, Mn^{II} yellow, O red, C black, Na orange.

and the octanuclear Ba clusters $[Ba_8O_2]^{12+}$, $[Sr_6Ba_2O_2]^{12+}$ and $[Ba_8Eu_2O_2]^{12+}$, where the principle bridging ligand is also an alkoxide group.[7] Similar cores are also found in the decanuclear complexes $[Fe_{10}O_2Cl_8(tmp)_6]$, $[(VO)_2Fe_8O_2Cl_6(tmp)_6]$ and $(NEt_4)_2[Mn_{10}O_2Cl_8(thme)_6]$.[8,9]

The magnetic properties of **1–3** were investigated by solid state magnetic susceptibility (χ_M) measurements in the 5.0–300 K temperature range and in dc fields up to 7 Tesla. The data are essentially identical for all three compounds. For **1**, $\chi_M T$ steadily decreases from 31.4 cm^3 K mol^{-1} at 300 K to 19.1 cm^3 K mol^{-1} at 20 K, and then decreases to 10.1 cm^3 K mol^{-1} at 5 K (Fig. 2). The data strongly suggest predominantly antiferromagnetic exchange interactions. Each complex contains eight Mn^{II} and four Mn^{III} ions with total spin values ranging from 0 to 28. Given the size of the molecules, it is not possible to apply the Kambe method to determine the individual pairwise exchange interaction parameters between the Mn ions, and direct matrix diagonalization methods are also computationally unfeasible. Thus, to determine the ground state spin of the complex, magnetization data were collected in the magnetic field and temperature ranges of 0.1–7 T and 1.8–4.0 K. However, we could not obtain a good fit for the data assuming that only the ground state is populated in this temperature range, suggesting that low-lying excited states are populated even at these low temperatures. In an additional effort to determine the ground state spin, ac susceptibility measurements were performed with a 3.5 G ac field oscillating at 500 Hz. The ac data are essentially superimposable with the dc data and appear to be heading for $\chi_M T \approx 6$ cm^3 K mol^{-1} at 0 K (Fig. 2), consistent with a small ground state spin value of $S \approx 3$, before a steeper drop at <3 K. The steeply sloping $\chi_M' T$ *vs.* T plot over a relatively narrow temperature range is characteristic of low-lying excited states with S greater than that of the ground state and which are increasingly populated as the temperature increases. This is completely consistent with the high content in the complex of Mn^{II} ions, which almost always give weak, antiferromagnetic exchange interactions.

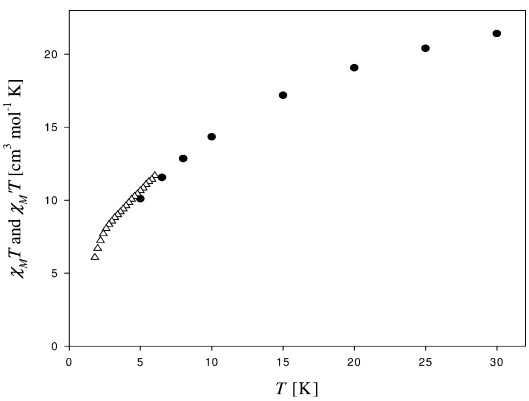

Fig. 2 Plot of the dc $\chi_M T$ *vs.* T data (●) for complex **1** in the 5.0–30 K temperature range, and the $\chi_M' T$ *vs.* T data in the 1.8–6.0 K range from ac susceptibility measurements (△).

In order to probe possible SMM behaviour, single-crystal magnetization *vs.* applied dc field sweeps were performed for complexes **1–3** at various field sweep rates and temperatures using a micro-SQUID apparatus,[10] and the obtained data are presented in Fig. 3. Hysteresis loops were observed whose coercivity was strongly temperature and sweep rate dependent, increasing with decreasing temperature and increasing field sweep rate, as expected for the superparamagnetic-like behaviour of a SMM. Both **1** and **3** exhibit broad, poorly-resolved steps due to quantum tunnelling of

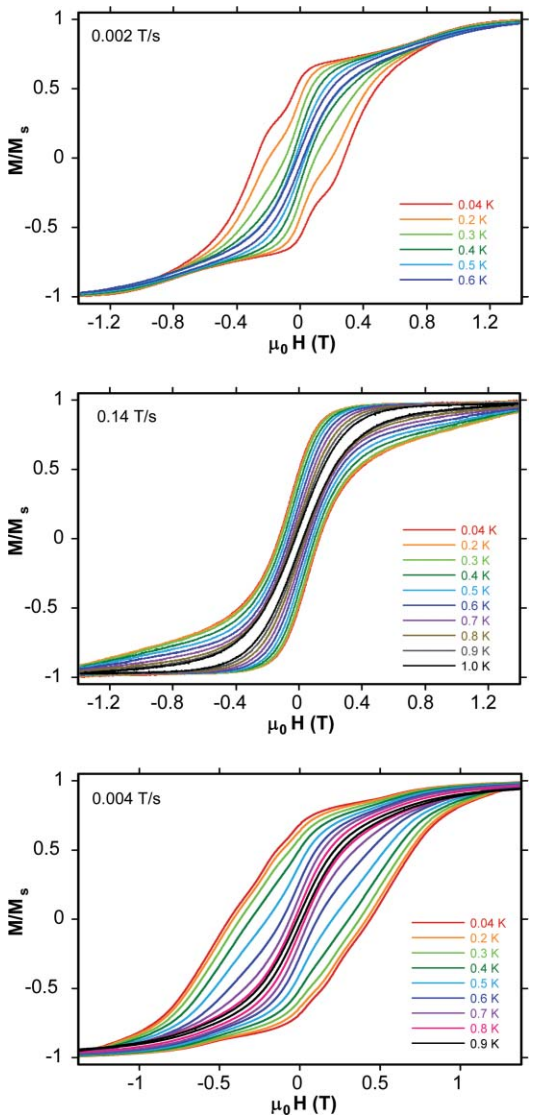

Fig. 3 Single crystal magnetisation (M) *vs.* field (H) hysteresis loops for complexes **1** (top), **2** (middle) and **3** (bottom) at the indicated field sweep rates and temperatures; the magnetisation is normalised to its saturation value (M_S).

magnetization (QTM), and **2** none at all, probably due primarily to step-broadening effects from the low-lying excited states, as well as distributions of local environments owing to ligand and solvent disorder, and weak intermolecular interactions.[4,5,11] Magnetization *vs.* time decay data were collected on **3**, which has the slowest relaxation at zero field, and used to construct an Arrhenius plot (Fig. 4); fitting of the thermally activated region to the Arrhenius equation $\tau = \tau_0 \exp(U_{eff}/kT)$ gave $U_{eff} = 13.9$ K and $\tau_0 = 1.4 \times 10^{-8}$ s, where U_{eff} is the effective relaxation barrier.

In conclusion, the combination of a reductive aggregation route and a tripodal chelate has led to a new family of $Mn^{III}_4Mn^{II}_8$ SMMs whose structures are derived from edge-sharing bioctahedra. The same product is obtained using a Mn^{II} reagent, indicating this to be the preferred [Mn_{12}] oxidation level under these conditions. Complex **3** has a chain-like structure, although intermolecular interactions are not expected to be strong through a diamagnetic Na^+ ion, and the complex is magnetically similar to **1** and **2**.

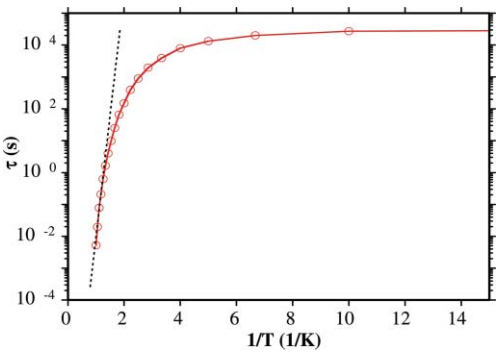

Fig. 4 Arrhenius plot for **3**; the dashed line is the fit of the thermally-activated region to the Arrhenius equation.

Notes and references

† Anal. (%). Calc. (found) for **1**·MeCN $C_{166}H_{163}Mn_{12}NO_{42}$: C, 56.91 (56.21); H, 4.68 (4.56); N, 0.40 (0.31). Anal. (%). Calc. (found) for **2**·MeCN·2H_2O ($C_{162}H_{169}Mn_{12}O_{44}N$): C, 55.69 (55.50); H, 4.87 (4.57); N, 0.40 (0.38). Anal. (%). Calc. (found) for **3**·1.5MeCN·10H_2O ($C_{46}H_{103.5}Mn_{12}NaNO_{55}$): C, 24.66 (24.31); H, 4.66 (4.38); N, 0.93 (0.90). *Crystal data.* **1**·6MeCN: $M_r = 3708.52$, orthorhombic, space group *Pbca*, $a = 28.4275(19)$, $b = 20.2935(14)$, $c = 29.446(2)$ Å, $Z = 4$, $V = 16987(2)$ Å^3, $D_c = 1.450$ g cm^{-3}, $T = 173(2)$ K. **2**·12MeCN: $M_r = 3908.82$, monoclinic, space group $P2_1/c$, $a = 20.5435(15)$, $b = 18.8989(14)$, $c = 25.3111(19)$ Å, $\beta = 111.180(2)°$, $Z = 2$, $V = 9163.2(12)$ Å^3, $D_c = 1.417$ g cm^{-3}, $T = 173(2)$ K. **3**·4MeCN: $M_r = 2226.57$, triclinic, space group $P\bar{1}$, $a = 11.5832(6)$, $b = 13.4283(8)$, $c = 14.0099(8)$ Å, $\alpha = 103.462(2)$, $\beta = 97.904(2)$, $\gamma = 90.706(2)°$, $Z = 2$, $V = 2096.9(2)$ Å^3, $D_c = 1.763$ g cm^{-3}, $T = 173(2)$ K. The structures were solved by direct methods in SHELXTL6 and refined on F^2 by full-matrix least squares. Final refinement parameters $R1$ ($wR2$) were 7.62 (14.22), 6.16 (17.70) and 4.26 (11.79) %, respectively ($I > 2\sigma(I)$). CCDC reference numbers 290612–290614. For crystallographic data in CIF or other electronic format see DOI: 10.1039/b517108c

1 R. Sessoli, H.-L. Tsai, A. R. Schake, S. Wang, J. B. Vincent, K. Folting, D. Gatteschi, G. Christou and D. N. Hendrickson, *J. Am. Chem. Soc.*, 1993, **115**, 1804.
2 G. Christou, D. Gatteschi, D. N. Hendrickson and R. Sessoli, *MRS Bull.*, 2000, **25**, 66.
3 G. Christou, *Polyhedron*, 2005, **24**, 2065, and references therein.
4 (*a*) M. Murugesu, M. Habrych, W. Wernsdorfer, K. A. Abboud and G. Christou, *J. Am. Chem. Soc.*, 2004, **126**, 4766; (*b*) M. Soler, W. Wernsdorfer, K. A. Abboud, J. C. Huffman, E. R. Davidson, D. N. Hendrickson and G. Christou, *J. Am. Chem. Soc.*, 2003, **125**, 3576; (*c*) J. B. Vincent, C. Christmas, H.-R. Chang, Q. Li, P. D. W. Boyd, J. C. Huffman, D. N. Hendrickson and G. Christou, *J. Am. Chem. Soc.*, 1989, **111**, 2086; (*d*) E. Bouwman, M. A. Bolcar, E. Libby, J. C. Huffman, K. Folting and G. Christou, *Inorg. Chem.*, 1992, **31**, 5185.
5 (*a*) A. J. Tasiopoulos, A. Vinslava, W. Wernsdorfer, K. A. Abboud and G. Christou, *Angew. Chem., Int. Ed.*, 2004, **43**, 2117; (*b*) A. J. Tasiopoulos, W. Wernsdorfer, K. Abboud and G. Christou, *Angew. Chem., Int. Ed.*, 2004, **43**, 6338; (*c*) A. J. Tasiopoulos, W. Wernsdorfer, K. A. Abboud and G. Christou, *Inorg. Chem.*, 2005, **44**, 6324; (*d*) P. King, W. Wernsdorfer, K. A. Abboud and G. Christou, *Inorg. Chem.*, 2005, **44**, 8659.
6 E. K. Brechin, *Chem. Commun.*, 2005, 5141.
7 (*a*) K. G. Caulton, M. H. Chisholm, S. R. Drake, K. Folding and J. C. Huffman, *Inorg. Chem.*, 1993, **32**, 816; (*b*) W. J. Evans, D. G. Giarikos, M. A. Greci and J. W. Ziller, *Eur. J. Inorg. Chem.*, 2002, 453.
8 M. I. Khan and J. Zubieta, *Prog. Inorg. Chem.*, 1995, **43**, 1.
9 (*a*) R. C. Finn and J. Zubieta, *J. Cluster Sci.*, 2000, **11**, 461; (*b*) M. Cavaluzzo, Q. Chen and J. Zubieta, *J. Chem. Soc., Chem. Commun.*, 1993, 131.
10 W. W. Wernsdorfer, *Adv. Chem. Phys.*, 2001, **118**, 99.
11 (*a*) E. Brechin, C. Boskovic, W. Wernsdorfer, J. Yoo, A. Yamaguchi, C. Sanudo, T. Concolino, A. Rheingold, H. Ishimoto, D. Hendrickson and G. Christou, *J. Am. Chem. Soc.*, 2002, **124**, 9710; (*b*) M. Murugesu, J. Raftery, W. Wernsdorfer, G. Christou and E. K. Brechin, *Inorg. Chem.*, 2004, **43**, 4203.